Seed Science Research (2006) **16**, 243–250 DOI: 10.1017/SSR2006257

Computational analysis of rice (*Oryza sativa* L.) panicle topology and ripening

Jordan O. Hay and Roger M. Spanswick*

Department of Biological and Environmental Engineering, Cornell University, Ithaca, New York 14853-5701, USA

Abstract

The processes involved in rice (*Oryza sativa* L.) panicle ripening vary with time and topological grain position. Methods to describe the functioning and connectivity of the grains on a panicle could aid the analysis of these processes. Hence, we addressed the difficulty of encoding and representing panicle topology. Array-based decomposition and computational methods were developed to encode and analyse panicle topology and grain traits. The technique, applied to the analysis of dry matter accumulation, clearly represented the basipetal succession of asynchronous grain ripening on a panicle. These methods should be useful for the spatial and temporal analysis of a number of panicle processes and attributes, including molecular ones, involved with ripening.

Keywords: caryopsis, computational analysis, grain filling, *Oryza sativa*, panicle architecture, panicle topology, rice

Introduction

In the rice (*Oryza sativa* L.) life cycle, spikelets of a panicle differentiate, develop, emerge, undergo pollination and fertilization, and finally form grains (Hoshikawa, 1989, 1993). Ripening, the process after double fertilization by which the caryopsis matures within the grain, varies with position on the panicle.

Apical growth and branching contribute to the formation of panicle topology, the pattern of branching that determines the number and position of grains in the panicle. There are typically three degrees of branching (Xu and Vergara, 1986; Takeoka *et al.*, 1993; Komatsu *et al.*, 2001). Primary (1°) branches are borne at rachis (panicle axis) nodes, secondary (2°) branches are borne at nodes on 1° branches, and spikelet pedicels are borne on 1° and 2° branches. Komatsu *et al*. (2001) classified the meristems that generate this topology as the primary inflorescence meristem, rachis branch meristems, lateral spikelet meristems and terminal spikelet meristems, and showed that meristem formation and specification are regulated by the genes *LAX1* and *FZP2*.

Differentiation and development of panicle primordia, spikelet flowering and grain ripening are asynchronous (Xu and Vergara, 1986). For instance, asynchronous differentiation of rachis branch meristem from the primary inflorescence meristems is acropetal. In contrast, asynchronous rachis branch development (acropetal differentiation of rachis branch meristems and/or spikelet meristems) progresses basipetally. Asynchronous differentiation of spikelet meristems from a single rachis branch meristem is acropetal. However, spikelet development (acropetal differentiation of spikelet organ primordia) progresses from the apical spikelet to the basal one, and then to the middle ones in acropetal order. Accordingly, spikelets flower asynchronously.

Topological variation in ripening involves more than asynchronous flowering, because ripening processes proceed differentially among grain positions. Distal and proximal grain positions differ in dry matter accumulation, starch accumulation, sucrose accumulation, amino acid accumulation, water accumulation, dehydration (Mohapatra *et al.*, 1993), gene expression (Ishimaru *et al.*, 2005), enzyme activity (Patel and Mohapatra, 1996; Ishimaru *et al.*, 2005), protein accumulation, soluble sugar accumulation (Mitra and Bera, 2003), abscisic acid accumulation (Tsukaguchi *et al.*, 1999), endosperm development, maternal tissue development (Ishimaru *et al.*, 2003), and in grain abortion and spikelet sterility (Xu and Vergara, 1986).

As sucrose is partitioned to the endosperm and stored as starch, dry matter accumulates in the caryopsis. Long- and short-distance transport of

*Correspondence
Fax: +1 607 255 4080
Email: rms6@cornell.edu

sucrose, the translocated form of sugar in rice (Fukumorita and Chino, 1982; Chino *et al.*, 1987), is accommodated by maternal phloem and plasmodesmata, respectively. Symplast discontinuity between maternal tissues and endosperm requires that sucrose molecules cross the plasma membranes (Oparka and Gates, 1981a, b). Accordingly, expression of the sucrose transporter *OsSUT1* occurs at the interface of the maternal nucellus and embryonic aleurone layer and reaches a maximum during mid-ripening (Hirose *et al.*, 1997, 2002; Furbank *et al.*, 2001). Furthermore, antisense expression of *OsSUT1* impairs dry matter accumulation (Scofield *et al.*, 2002). Temporal patterns of activity and expression of the cell wall invertase OsCIN1 suggest that monosaccharide transport is important during early caryopsis growth (Hirose *et al.*, 2002).

Encoding and representing topology facilitates the study of processes with respect to the connections between organs (Godin, 2000). We asked whether computational analysis would be useful for the representation of panicle topology and asynchronous and differential processes involved with ripening. Our approach used Matlab® and avoided manual drawings, analyses of grains from a small number of positions and computation using spreadsheets. Arrays and graphs that encoded and represented panicle topology described the basipetal progression of dry matter accumulation and should be useful for the topological analysis of other grain characteristics, even at the molecular level.

Materials and methods

Plant cultivation

Rice (*Oryza sativa* L., cv. Jefferson) was grown in a greenhouse according to Hay and Spanswick (2006). Six sets of panicles were harvested. Sets 1–3 each contained five panicles that emerged first on a plant and were harvested 10, 15 and 20 d after emergence (DAE), respectively. No other panicles were removed from these plants. Sets 4–6 each contained eight panicles that emerged first, third and fifth respectively, and were harvested at maturity. Set 7 designated the combination of sets 1–6 (39 panicles). Harvested panicles were dried at room temperature to a constant weight before they were analysed.

Computational analysis

An approach that encoded grain connectivity and features related to ripening in a way compatible for analysis in Matlab® (The Mathworks Inc., Natick, Massachusetts, USA) was conceived. The procedure consisted of five distinct steps: (1) First, the grains were detached from the panicle and placed sequentially in the wells of 96-well plates, with topological information indicated by the number of empty wells left between the grains. (2) The information was converted to a numerical array for entry into Matlab®. (3) The array was converted to a more compact form. (4) A procedure was implemented to produce a consensus array from all the panicles in a sample. (5) Finally, the array was displayed in diagrammatic form and/or information was expressed graphically.

In the first step, grains on a panicle were indexed in acropetal order according to the example in Fig. 1a. So that grain attributes could be measured for each position on the panicle, grains were detached in acropetal order and arrayed on 96-well plates from left to right and bottom to top. Wells were skipped during the arraying process in order to encode topological information. If the first rachis node had only 1° grains, 1° and 2° grains, or no grains, the first three, four, or five wells were skipped, respectively, before the first grain was arrayed. This took into account panicles that did not have a rachis branch associated with the first rachis node (neck node). Other wells were skipped in a way that was related to panicle topology (Table 1) to encode information on grain connectivity.

To demonstrate how this array procedure could be used to relate panicle topology to ripening processes, dry matter accumulation was assessed in a qualitative way by filling the wells with water. Ones, twos and threes (chosen because of their proximity on a keyboard) were assigned to wells with a grain that sank, wells with a grain that floated and skipped wells respectively. The resulting sequence of numbers was then entered into Excel, saved as a tab-delimited text file, and imported into Matlab® as the panicle array (Fig. 1b).

In the third step, the panicle array (Fig. 1b) was computationally annotated to make it more easily interpretable. Sequences of threes were replaced with numbers ≥ 10 that indicated the topological position of the grains they bordered. The last digit of a border was used to indicate the 2° branch a grain was on (a zero was used for 1° grains) and the other digit(s) were used to indicate the rachis node a grain was associated with. For example, the borders for grains 4–8 and 12–17 (Fig. 1a) were 10 and 20, respectively (Fig. 1c). Similarly, the borders for grains 34–36 and 37–39 were 51 and 52, respectively (rachis nodes and 2° branches were indexed acropetally). Annotated panicle arrays (Fig. 1c) were manipulated to compute the values of various panicle traits (see Table 2) or traits as a function of rachis node (see Figs 2 and 4).

For the fourth step, generation of a consensus annotated panicle array, borders and zeros were inserted into annotated panicle arrays in a way that aligned all the borders. For instance, the alignment of

https://doi.org/10.1017/SSR2006257 Published online by Cambridge University Press

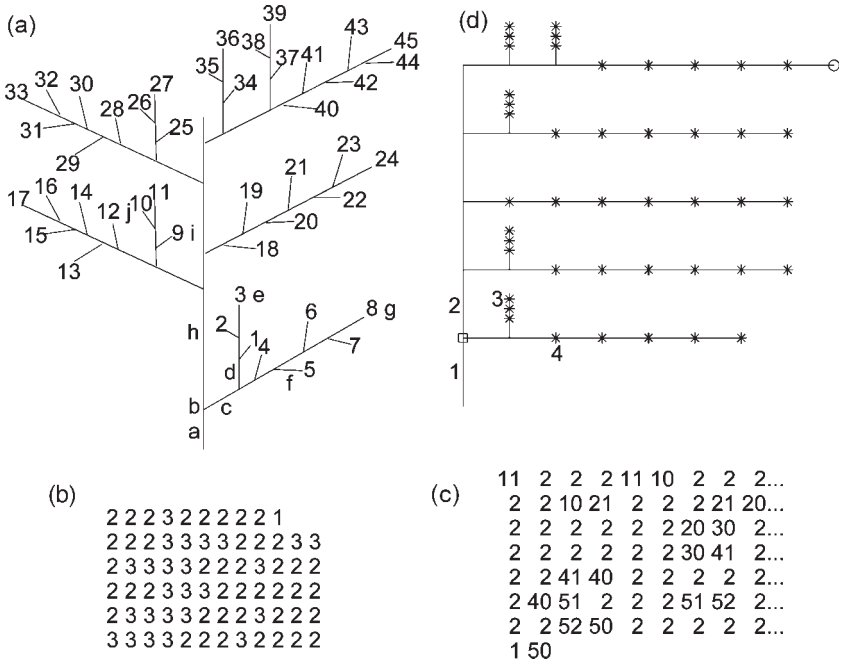

Figure 1. Encoding and representation of rice panicle topology with arrays and graphs. (a) Manual drawing of the proximal portion of a panicle. 1–45, grains indexed in acropetal order; a, peduncle; b, first rachis node; c, 1° (primary) branch; d, 2° (secondary) branch; e, apical 2° grain; f, pedicel; g, apical 1° grain; h, rachis; i, basal 2° grain; j (grain 12), basal 1° grain. (b) Panicle array representation of (a). 1, well with grain that sank; 2, well with grain that floated; 3, well that was skipped according to Materials and methods (initial sequence) and Table 1 (other sequences). The two-dimensional array is indexed from left to right and bottom to top. (c) Annotated panicle array. 1, grain that sank; 2, grain that floated; ≥10, borders. The last border digit indicates the 2° branch a grain was on (1° grains have a zero) and the other digit indicates the rachis node a grain was associated with. The one-dimensional array is indexed from left to right and top to bottom. (d) Panicle graph. *, grain that floated; ○ , grain that sank; □, first rachis node; 1, peduncle; 2, rachis; 3, 2° grain; 4, 1° grain.

10 2 2 1 2 10 20 1 1 2 2 20

and

10 2 2 2 10

is

10 2 2 1 2 10 20 1 1 2 2 20
10 2 2 2 0 10 20 0 0 0 0 20.

For consensus generation, a position was assigned a 0 (to represent the absence of a grain) if a grain (1 or 2) was present in <50% of the aligned annotated panicle arrays, a 1 (to represent a grain that sank) if it was present in ≥50% of the aligned annotated panicle arrays, or else a 2 (to represent a grain that floated). For instance, the consensus of the alignment

10 1 2 2 10
10 2 2 0 10
10 1 1 0 10
10 2 2 0 10
10 1 1 0 10
10 2 2 2 10

is

10 1 2 0 10.

Table 1. Relationship between rice panicle topology and the acropetal arraying of grains on 96-well plates. The transitions in the column labelled 'Example' refer to Fig. 1a. Threes in Fig. 1b designate skipped wells. These definitions do not apply to the initial group of skipped wells (see Materials and methods)

Step from	Step to	Example	Number of wells skipped
Grain	Next grain (same branch)	1 → 2	0
Apical 2° grain	Basal 1° grain (same rachis node)	3 → 4	1
Apical 2° grain	Basal 2° grain (same rachis node)	36 → 37	2
Apical 1° grain	Basal 1° grain (next rachis node)	17 → 18	3
Apical 1° grain	Basal 2° grain (next rachis node)	8 → 9	4

https://doi.org/10.1017/SSR2006257 Published online by Cambridge University Press

Table 2. Rice panicle traits. Averages (μ) and 95% confidence intervals ($\pm$) are listed. See Materials and methods for the description and sample size of each panicle set

Trait		Set 1	Set 2	Set 3	Set 4	Set 5	Set 6	Set 7
Rachis nodes	μ	16.00	16.20	14.20	15.00	13.88	13.25	14.59
	±	0.88	2.04	1.62	0.89	0.54	1.40	0.51
Grains	μ	186.20	177.80	163.60	145.38	133.88	117.75	149.08
	±	26.77	17.19	30.28	8.94	8.61	18.77	9.40
1° Grains	μ	96.40	95.60	84.40	86.38	78.75	74.00	84.49
	±	6.43	13.36	10.77	5.99	3.97	9.47	3.64
1° Branches	μ	15.80	16.20	14.00	15.00	13.75	13.13	14.49
	±	0.56	2.04	1.52	0.89	0.39	1.37	0.50
1° Grains/ 1° branch	μ	6.10	5.90	6.02	5.76	5.72	5.63	5.82
	±	0.33	0.26	0.22	0.13	0.17	0.22	0.08
2° Grains	μ	89.80	82.20	79.20	59.00	55.13	43.75	64.59
	±	23.45	11.36	23.39	5.53	7.72	12.04	6.60
2° Branches	μ	28.80	25.80	24.60	19.25	17.88	14.75	20.79
	±	6.54	3.21	7.43	1.66	2.16	3.73	1.96
2° Grains/ 2° branch	μ	3.11	3.18	3.22	3.06	3.08	2.94	3.08
	±	0.10	0.06	0.09	0.05	0.09	0.13	0.04

Finally, the zeros were removed, and the resulting consensus annotated panicle array was graphed (Fig. 1d) with symbols that represented the grains and their character states. Procedures for graphical display of panicle traits were also devised (see Figs 2 and 4).

The toolbox of Matlab® functions is based on Hay (2005). It is available at URL: http://hdl.handle.net/1813/3105, together with a demonstration Matlab® program to illustrate how the functions may be used, and data files that may be used to reproduce the figures in this paper.

Results

Panicle topology

Panicles had three orders of branching. Table 2 shows the average values of various panicle traits. For set 7 panicles, the rachis had c. 15 nodes and almost the same number of 1° branches (sometimes there was not a 1° branch at the first rachis node). Panicles had more 2° branches and fewer 2° grains than 1° ones. The ratio of 2° branches to 1° branches, 1° grains to 2° grains, and grains per 1° branch to grains per 2° branch was 1.4, 1.3 and 1.9, respectively. The number of rachis nodes, grains and branches all decreased with order of panicle emergence (compare sets 4–6), but not DAE (sets 1–3).

Panicle traits varied with rachis node (Fig. 2). The number of grains, 2° grains and 2° branches as a function of node increased, reached a maximum at nodes 6–7, and decreased. The nodal distribution of number of 1° grains was comparatively constant.

The consensus panicle graph (Fig. 3) displayed a similar nodal distribution of grains and branches. There were six grains per 1° branch except for the distal ones, which had four or five. The number of grains and 2° branches varied across 15 rachis nodes. Nodes 5–11 had more grains and 2° branches than the other nodes. Secondary branches typically had three grains. Rachis nodes had a maximum of two 2° branches. The first, fourteenth and fifteenth rachis node did not have 2° branches.

Panicle ripening

The proportion of grains that were dense varied with rachis node and DAE (Fig. 4). At least 50% were dense for all rachis nodes of panicles 20 DAE. Panicles 10 and 15 DAE did not have dense grains at the lower rachis nodes. More rachis nodes lacked dense grains for panicles 10 DAE than 15 DAE. For panicles 10, 15 and 20 DAE, dense grains were more numerous on upper rachis nodes than lower ones. The nodal distribution of dense grains was more similar to that of dense 1° grains than 2° grains.

Consensus panicle graphs showed similar spatial and temporal variation in grain density (Fig. 5). Dense grains were absent, the minority, and the majority for panicles 10, 15, and 20 DAE, respectively. For panicles 15 DAE, most of the dense grains were 1° grains of upper rachis nodes.

Discussion

Encoding and representing panicle topology

Our analysis of panicle topology deals with grain connectivity, not shape or spatial orientation. Methods based on constraints on panicle branching were developed for the indexing and decomposition of

https://doi.org/10.1017/SSR2006257 Published online by Cambridge University Press

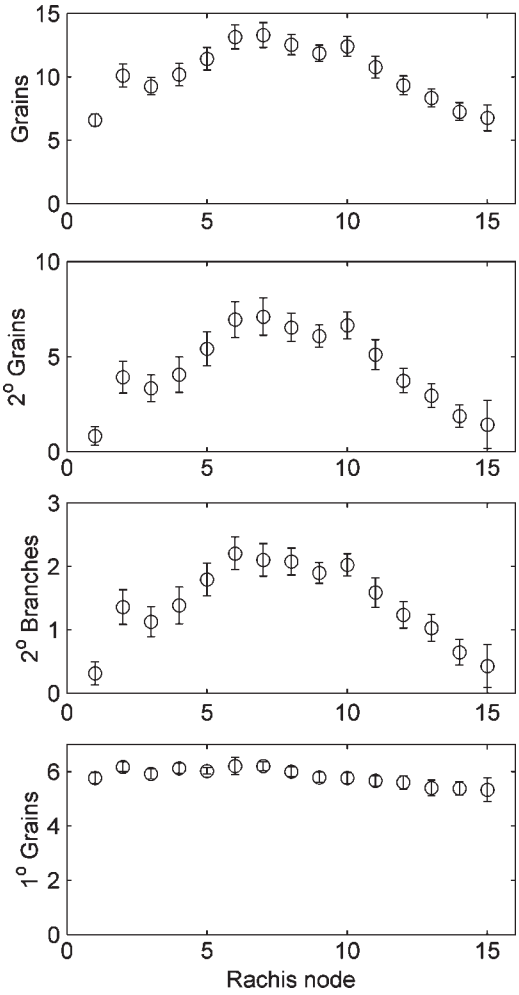

Figure 2. Distribution of traits among rachis nodes of all rice panicles sampled. Number of grains and branches of panicles in set 7 are plotted as a function of the first 15 rachis (panicle axis) nodes (indexed acropetally). Bars are the 95% confidence interval of a mean of 35 (node 1), 39 (nodes 2–11), 38 (node 12), 35 (node 13), 31 (node 14) or 21 (node 15) replicates (panicles that had grains at the given node).

grains on a panicle. The main difficulty in indexing grains is that rachis internodes can be very short. For instance, with ideal growth conditions during the panicle differentiation stage, two or three rachis branches are commonly found near the junction between peduncle and rachis (Matsushima, 1967).

Our method for decomposing the panicle involves arraying grains in order on 96-well plates according to rules for skipping wells. The main advantage of this method is that it encodes information on grain connectivity. That is, the plates of arrayed grains actually represent panicle topology. In addition, the character state of a trait can be easily determined for each grain. Since the grains are in wells, measurements

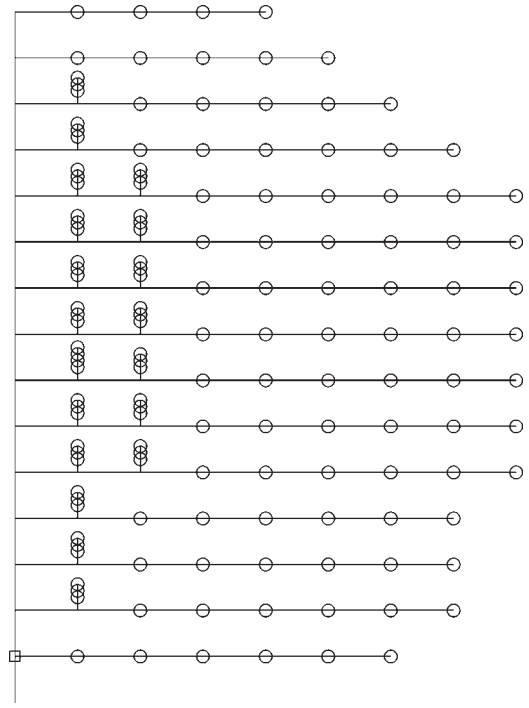

Figure 3. Consensus graph of all sampled rice panicles. The consensus annotated array of panicles in set 7 was graphed. ○, grain; □, first rachis node.

that require an aqueous environment can be made. As a most basic example, a single, qualitative trait (sinking versus floating in water) was assessed. However, more advanced techniques, such as genetic and biochemical ones, could be used for the analysis of multiple qualitative and quantitative traits. Another advantage of this method is that a numerical array representation of the 96-well plates can be entered into a spreadsheet with little effort. This is especially true for the analysis of a qualitative trait where there are only three types of wells, empty (skipped) ones and ones that contain a grain with either character state. Thus, the panicle array (Fig. 1b) is a numerical representation of both grain connectivity and attributes.

The major disadvantage of the panicle array is that it is difficult to interpret visually. Computational annotation of the panicle array is a solution to this problem. Borders demarcate values of grain traits according to rachis branch. There are many advantages to the annotated array representation of a panicle. First, it encodes topology and grain attributes, and is compatible with array manipulations in Matlab®. Grain traits as a function of rachis node (Figs 2 and 4) or individual grain position can be assessed easily. Secondly, it can be represented by a panicle graph (Fig. 1d), eliminating the need for manual drawings of panicles. The panicle graph is a graph that has grain attributes superimposed on it.

https://doi.org/10.1017/SSR2006257 Published online by Cambridge University Press

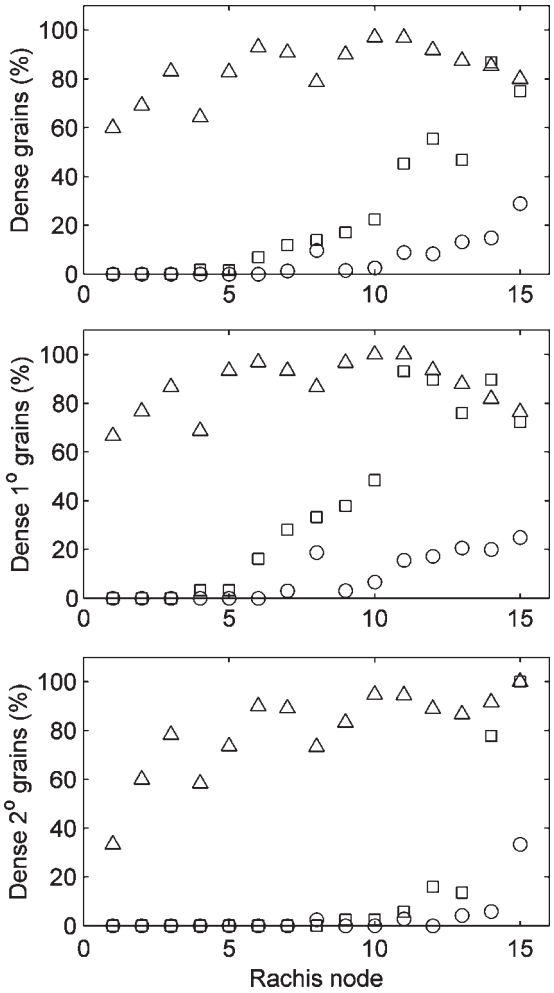

Figure 4. Distribution of dense grains among rachis nodes of rice panicles sampled at various days after emergence. ○, 10 DAE (set 1); □, 15 DAE (set 2); Δ, 20 DAE (set 3). Symbols are the mean number of dense grains (1° plus 2°, 1° or 2°) divided by the mean number of grains (1° plus 2°, 1° or 2°) multiplied by 100. Means are of 3 (20 DAE node 15), 4 (10 DAE node 1 and 20 DAE nodes 1, 13–14), or else 5 replicates (panicles that had grains at the given node).

Compared to the arrays, it is a superior visual representation of grain connectivity and functioning. Finally, the arrays can be easily aligned. In this way, a consensus array, which smoothes out panicle-to-panicle variation, can be determined.

Analysis of panicle topology

The output of this computational analysis clearly presents the topology of the panicle. A strength of the output is that it reveals the nature of the panicle on average. The variation in topology and traits was smoothed out in two ways. The first was by manipulating a set of annotated panicle arrays to extract data, such as number of grains as a function of rachis node, from each and then computing averages. The second was by computing the consensus array and analysing its graph. From both types of analysis, it is clear that, at the level of the panicle, there is nodal variation of quantitative traits. Secondary branches were more numerous at the middle rachis nodes (Fig. 2) and varied little in the number of grains (Fig. 3). The nodal distribution of number of grains was thus more similar to that of 2° grains than that of 1° ones (Fig. 2). Because vestiges were not considered, the nodal distributions of panicle traits only approximate actual panicle differentiation. Nodal distributions, especially for 2° branches and spikelets, can be different when vestiges are taken into account (Kobayasi and Imaki, 1997). Panicles can be classified morphologically on the basis of which nodes have the most 2° spikelets (Takeoka *et al.*, 1993). The cultivar Jefferson has 2° branches associated more frequently with the middle nodes of the rachis (Figs 2, 3). These methods may be useful for comparative panicle topology in the context of natural variation or physiological or genetic manipulations.

Analysis of the spatial and temporal dynamics of panicle ripening

The output also clearly presents the asynchronous ripening of grains on the panicle. The positional variation in the qualitative character state of grain density was captured by taking advantage of the fact that a grain sinks when the caryopsis fills enough of the air space enclosed by the hull. The general basipetal progression of panicle ripening with rachis node is obvious (Figs 4, 5). Distal 1° grain positions are superior in terms of the time after panicle emergence it takes for the caryopsis to ripen enough to make the grain dense.

Conclusion

A computational approach to the analysis of the relationship between panicle topology and ripening has been established. An analysis of the positional and temporal variation in dry matter accumulation was presented. Interesting questions arise, such as the extent of the variation of gene expression and protein activity. Qualitative and quantitative measures of these processes could be determined for each spikelet/grain on the panicle at different times before and after emergence and presented as a function of rachis node or position on the panicle. Hence, these methods could lead to a better understanding of how

https://doi.org/10.1017/SSR2006257 Published online by Cambridge University Press

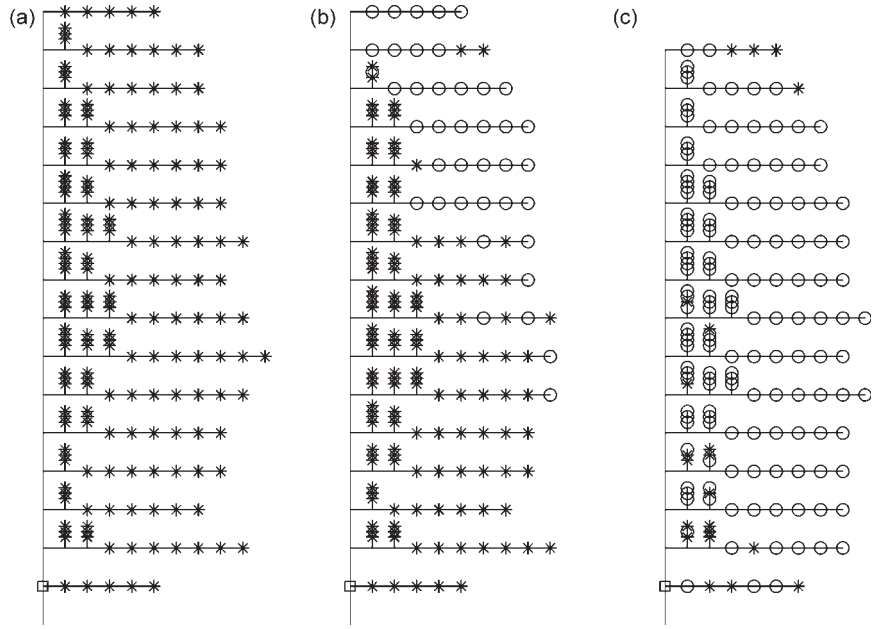

Figure 5. Consensus graph of rice panicles sampled at various days after emergence. (a) 10 DAE (set 1). (b) 15 DAE (set 2). (c) 20 DAE (set 3). *, grain that floated; ○, grain that sank; □, first rachis node.

panicle ripening varies at the molecular level in both space and time.

Acknowledgements

The authors thank the College of Agriculture and Life Sciences for support, Kyoungeun Song for technical assistance, Professor Larry Walker for advocating the application of Matlab® and Professor Susan McCouch for helpful discussion.

References

Chino, M., Hayashi, H. and Fukumorita, T. (1987) Chemical composition of rice phloem sap and its fluctuation. *Journal of Plant Nutrition* **10**, 1651–1661.

Fukumorita, T. and Chino, M. (1982) Sugar, amino acid and inorganic contents in rice phloem sap. *Plant and Cell Physiology* **23**, 273–283.

Furbank, R.T., Scofield, G.N., Hirose, T., Wang, X.D., Patrick, J.W. and Offler, C.E. (2001) Cellular localisation and function of a sucrose transporter *OsSUT1* in developing rice grains. *Australian Journal of Plant Physiology* **28**, 1187–1196.

Godin, C. (2000) Representing and encoding plant architecture: a review. *Annals of Forest Science* **57**, 413–438.

Hay, J.O. (2005) Growth, architecture, cell separation, electrophysiology and sucrose transport of ripening rice caryopses. PhD dissertation, Cornell University, Ithaca, New York, USA.

Hay, J.O. and Spanswick, R.M. (2006) Mechanical and enzymatic separation of ripening rice (*Oryza sativa* L.) caryopsis tissues. *Seed Science Research* **16**, 223–227.

Hirose, T., Imaizumi, N., Scofield, G.N., Furbank, R.T. and Ohsugi, R. (1997) cDNA cloning and tissue specific expression of a gene for sucrose transporter from rice (*Oryza sativa* L.). *Plant and Cell Physiology* **38**, 1389–1396.

Hirose, T., Takano, M. and Terao, T. (2002) Cell wall invertase in developing rice caryopsis: molecular cloning of *OsCIN1* and analysis of its expression in relation to its role in grain filling. *Plant and Cell Physiology* **43**, 452–459.

Hoshikawa, K. (1989) *The growing rice plant: An anatomical monograph*. Tokyo, Nobunkyo.

Hoshikawa, K. (1993) Anthesis, fertilization and development of caryopsis. pp. 339–376 *in* Matsuo, T.; Hoshikawa, K. (Eds) *Science of the rice plant*. Tokyo, Food and Agricultural Policy Research Center.

Ishimaru, T., Matsuda, T., Ohsugi, R. and Yamagishi, T. (2003) Morphological development of rice caryopses located at the different positions in a panicle from early to middle stage of grain filling. *Functional Plant Biology* **30**, 1139–1149.

Ishimaru, T., Hirose, T., Matsuda, T., Goto, A., Takahashi, K., Sasaki, H., Terao, T., Ishii, R., Ohsugi, R. and Yamagishi, T. (2005) Expression patterns of genes encoding carbohydrate-metabolizing enzymes and their relationship to grain filling in rice (*Oryza sativa* L.): comparison of caryopses located at different positions in a panicle. *Plant and Cell Physiology* **46**, 620–628.

Kobayasi, K. and Imaki, T. (1997) Varietal differences of rice in differentiation and degeneration of secondary rachis-branches and spikelets in terms of their nodal

https://doi.org/10.1017/SSR2006257 Published online by Cambridge University Press

distribution on a rachis. *Japanese Journal of Crop Science* **66**, 578–587.

Komatsu, M., Maekawa, M., Shimamoto, K. and Kyozuka, J. (2001) The *LAX1* and *FRIZZY PANICLE 2* genes determine the inflorescence architecture of rice by controlling rachis-branch and spikelet development. *Developmental Biology* **231**, 364–373.

Matsushima, S. (1967) *Crop science in rice: Theory of yield determination and its application*. Tokyo, Fuji Publishing.

Mitra, S. and Bera, A.K. (2003) Influence of grain density on some qualitative characters of rice (*Oryza sativa* L.). *Crop Research* **25**, 400–405.

Mohapatra, P.K., Patel, R. and Sahu, S.K. (1993) Time of flowering affects grain quality and spikelet partitioning within the rice panicle. *Australian Journal of Plant Physiology* **20**, 231–241.

Oparka, K.J. and Gates, P. (1981a) Transport of assimilates in the developing caryopsis of rice (*Oryza sativa* L.): The pathways of water and assimilated carbon. *Planta* **152**, 388–396.

Oparka, K.J. and Gates, P. (1981b) Transport of assimilates in the developing caryopsis of rice (*Oryza sativa* L.): Ultrastructure of the pericarp vascular bundle and its connections with the aleurone layer. *Planta* **151**, 561–573.

Patel, R. and Mohapatra, P.K. (1996b) Assimilate partitioning within floret components of contrasting rice spikelets producing qualitatively different types of grains. *Australian Journal of Plant Physiology* **23**, 85–92.

Scofield, G.N., Hirose, T., Gaudron, J.A., Upadhyaya, N.M., Ohsugi, R. and Furbank, R.T. (2002) Antisense suppression of the rice sucrose transporter gene, *OsSUT1*, leads to impaired grain filling and germination but does not affect photosynthesis. *Functional Plant Biology* **29**, 815–826.

Takeoka, Y., Shimizu, M. and Wada, T. (1993) Panicles. pp. 295–338 *in* Matsuo, T.; Hoshikawa, K. (Eds) *Science of the rice plant*. Tokyo, Food and Agricultural Policy Research Center.

Tsukaguchi, T., Horie, T. and Koshioka, M. (1999) Dynamics of abscisic acid levels during grain-filling in rice: comparisons between superior and inferior spikelets. *Plant Production Science* **2**, 223–226.

Xu, X.B. and Vergara, B.S. (1986) Morphological changes in rice panicle development: a review of literature. *IRRI Research Paper Series* **117**, 1–13.

Received 19 September 2005
accepted after revision 25 July 2006